J|A|C|S COMMUNICATIONS

Published on Web 08/10/2010

Direct Imaging of Intermolecular Bonds in Scanning Tunneling Microscopy

Christian Weiss,[†,‡] Christian Wagner,[†,‡] Ruslan Temirov,[†,‡] and F. Stefan Tautz*[,†,‡]

Institut für Bio- und Nanosysteme 3, Forschungszentrum Jülich, 52425 Jülich, Germany and JARA-Fundamentals of Future Information Technology, 52425 Jülich, Germany

Received May 19, 2010; E-mail: s.tautz@fz-juelich.de

Abstract: Local, noncovalent intermolecular interactions in organic monolayers have been directly imaged using scanning tunneling hydrogen microscopy (STHM). Unprecedented spatial resolution directly reveals the relation between the intermolecular interactions, the molecular chemical structure, and the ordering in the film.

Molecular layers at surfaces form the basis of surface functionalization. It is therefore important to understand the principles behind their structural organization.[1] Molecular ordering at surfaces is controlled by the balance between molecule−substrate and intermolecular interactions. To allow tuning structures and functionalities, both types of interactions need to be understood. Molecule−substrate effects, such as covalent bonding, hybridization of molecular orbitals with substrate states, or charge transfer, can be studied spectroscopically, both on ensembles[2] and at the single molecule level.[3] In contrast, local intermolecular interactions, such as hydrogen bonding, are usually weaker and therefore more difficult to pinpoint. Nevertheless, their important role can be concluded indirectly from their profound influence on the lateral structure of molecular layers.[4] Unfortunately, such indirect arguments often leave ambiguities, and it is therefore desirable to find more direct evidence for the presence of local intermolecular bonds in molecular layers at surfaces.

In this communication we present images of molecular layers in which *local intermolecular bonds* appear directly and with remarkable clarity. The images have been recorded by scanning tunneling hydrogen microscopy (STHM). STHM is a special operation mode of a conventional low temperature scanning tunneling microscope in which molecular hydrogen or deuterium is condensed in the tunneling junction. It yields images corresponding more closely to the atomic structure of molecules, instead of their electronic structure.[5,6]

We have performed our experiments on various phases of the functionalized aromatic hydrocarbon molecule 3,4,9,10-perylene-tetracarboxylic-dianhydride (PTCDA) on Au(111). A model of the most stable phase, the so-called *herringbone phase*,[7,8] is shown in Figure 1a. Looking at the structure of the herringbone layer, it is clear that it is favored by the electrostatic interaction between the global quadrupole moments of neighboring molecules.[9] The presence or absence of hydrogen bonds, however, is not a priori clear.

Figure 1b shows an STM image of the herringbone phase. The molecules occur as bright and unstructured protrusions. In contrast, the STHM image (Figure 1c) reveals the atomic structure of the molecule, with the five rings of the perylene core appearing bright and the C_5O heterorings slightly darker.[5,6] Most importantly in the present context, a clear tile pattern which does not belong to the substrate is observed in the space between the molecules. Comparing this pattern with the molecular arrangement, we observe a remarkable coincidence between the tiles and the lines that connect oxygen atoms on one molecule to adjacent hydrogen atoms on neighboring molecules (Figure 1d). These are the positions at which one would expect hydrogen bonds. The number and location of the H-bonds identified

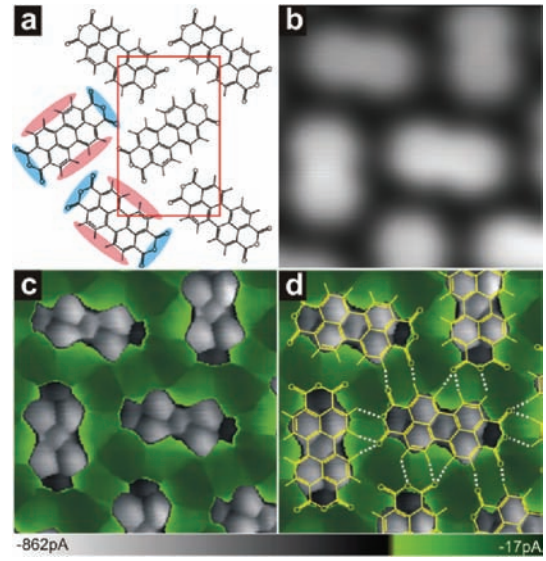

Figure 1. (a−d) Herringbone phase of PTCDA molecules on Au(111). (a) Structure model, lattice constants (12.3 × 19.2 Å^2) taken from ref 7, molecular orientation and structure in analogy to bulk β-PTCDA.[17] The molecular quadrupole moment and the unit cell are indicated. (b) Conventional STM image in constant height mode. (c) STHM image. A two-color palette has been used. (d) Superposition of the image from (c) with the structure of the herringbone phase in (a). White lines mark possible hydrogen bonds. Image parameters: (b) 25 × 25 Å^2, const. height, $V = 200$ mV; (c and d) 25 × 25 Å^2, const. height, $V = -2$ mV.

in Figure 1d correspond well to those found in a systematic theoretical search,[10] with one exception: the bonds involving the bridge oxygens.

The distances between oxygen atoms and closest hydrogen atoms on adjacent molecules in Figure 1d range from 1.9 to 2.6 Å, indicating rather weak O··H−C bonds of mainly an electrostatic nature.[11] Regardless of the physical origin of the contrast in Figure 1c, the image clearly indicates local interactions between the PTCDA molecules in the herringbone phase. Such local interactions are also expected independently of the present data from spectroscopic and structural evidence.[3,4,12]

We now turn to a second example for the remarkable STHM imaging capability regarding local interactions. Doping a sample of *PTCDA on Au(111)* with *potassium* leads to a partial reordering of the molecular layer from the herringbone to a square phase. Figure 2a, recorded on a sample with a 1:1 ratio of square and herringbone, shows the *K-induced square structure*, but no direct evidence for the presence of the dopant atoms is found in this STM image. Indeed, the image of the K-doped square phase (Figure 2a) is virtually identical to the image of the *square phase* of *pure PTCDA on Au(111)* (Figure 2d) that is occasionally found in small islands within the herringbone phase.[13] STM thus does not reveal where potassium is located in the potassium-induced structure, and consequently we cannot obtain any information from STM about the K-PTCDA interaction that stabilizes the K-doped square phase, thereby dramatically increasing its abundance compared to the pure square phase.

[†] Forschungszentrum Jülich.
[‡] JARA.

10.1021/ja104332t

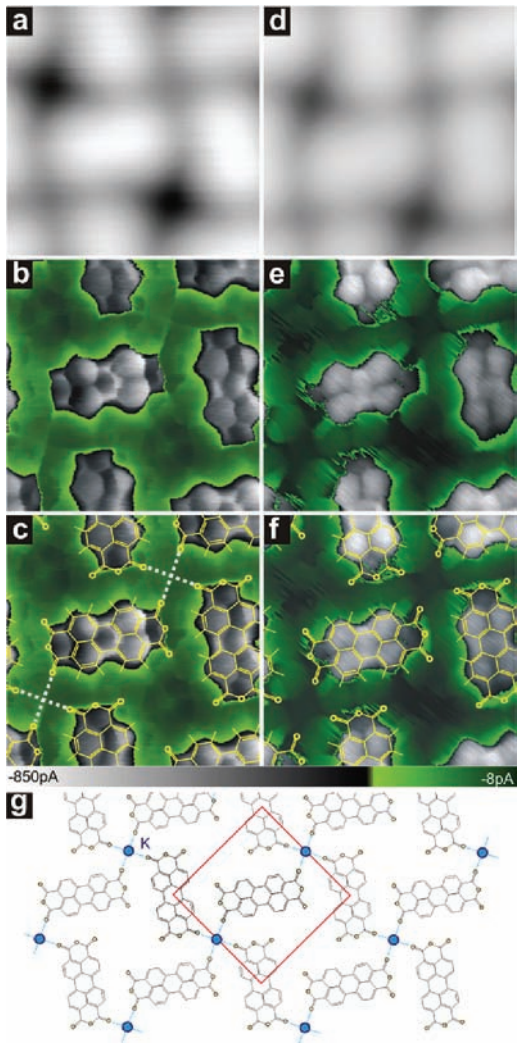

Figure 2. (a) STM image of K/PTCDA/Au(111) (24 × 24 Å^2, $I = 0.1$ nA, $V = 340$ mV). (b) STHM image of K/PTCDA/Au(111) (24 × 24 Å^2, const. height, $V = -2$ mV). (c) same as (b), but with structure formulas of PTCDA superimposed. Unit cell approximately $a_1 = a_2 = 16.0 \pm 0.5$ Å. White lines indicate O··K bonds visible in (b). (d) STM image of the PTCDA/Au(111) square phase (24 × 24 Å^2, $I = 0.1$ nA, $V = 314$ mV). (e) STHM image of the PTCDA/Au(111) square phase (24 × 24 Å^2, const. height, $V = -2$ mV). (f) same as (e), but with structure formulas of PTCDA superimposed. Unit cell approximately $a_1 = a_2 = 15.9 \pm 0.5$ Å. (g) Structure model of the 1:2 K/PTCDA/Au(111) phase in panels (a) to (c).

The situation is very different if STHM images are considered. In the STHM image of the K-doped phase (Figure 2b) we observe a remarkable feature in the small hollows between the molecules (upper right and lower left part of Figure 2b): Four thin, sharp lines extend from the corners of the adjacent molecules to the center of the hollow, forming a clover-leaf-like structure. From Figure 2c, in which the STHM contrast has been overlaid with structure formulas of PTCDA molecules, it becomes clear that these lines originate precisely at the corner oxygen atoms of the four PTCDA molecules surrounding the small hollow. Notably, the STHM image of the pure PTCDA/Au(111) square phase (Figure 2e) does not show these lines.

This finding suggests that potassium is located in the centers of the small hollows, at the positions where the lines meet and where potassium is 4-fold coordinated to the corner oxygen atoms of the four surrounding PTCDA molecules. Geometrically and chemically, this structure makes sense: Work function measurements on Au(100) have indicated that, at low concentrations, potassium is found in a positive ionic state on gold surfaces.[14] Given the ionic radius of potassium of ~1.5 Å[15]), and the van der Waals radius of oxygen of ~1.4 Å,[16] positively charged potassium ions fit very well into the small hollows of the K/PTCDA/Au(111) structure, because the distance between opposite oxygen atoms across the small hollow in our images is ~5.3 ± 0.5 Å. In contrast, the large hollows are too large for a coordinative bond which would have an O··K distance of 4.5 Å—and indeed the STHM image of Figure 2b does not show lines in the large hollows.

STHM images thus reveal a scenario in which each positively charged potassium ion interacts with the negative partial charges of four corner oxygen atoms (on four surrounding PTCDA molecules). Each PTCDA molecule in turn is bonded to two potassium ions. In this way, potassium stabilizes the 4-fold symmetric 1:2 K/PTCDA monolayer, and remarkably the K-PTCDA interactions which cause this stabilization are directly visualized in STHM. It is possible to estimate the corresponding interaction energy. According to ref 10, the square phase of undoped PTCDA has a 12% smaller intermolecular binding energy than the herringbone phase (1.18 eV vs 1.34 eV). The presence of K in the square phase should increase its binding energy by at least this amount, making it comparable to or higher than the binding energy of the herringbone phase with which the K-doped square phase coexists. This indicates a binding energy of ≳80 meV per O··K bond.

Interestingly, the potassium-free square phase shows an increased noise level in comparison with the herringbone phase in the same image (cf. the Supporting Information for a larger section of Figure 2e). Consistent with ref 10 which reports the existence of several energetically equivalent square phases of slightly different structure, this may indicate that PTCDA molecules in the open square structure lack lateral fixation if the stabilizing influence of potassium is missing.

In summary, we have demonstrated the capability of STHM to image local, noncovalent intermolecular interactions in two-dimensional molecular layers. In the present examples, both O··H—C and O··K bonds have been resolved, as thin lines or as sharp boundary lines between areas of different brightness. The physical origin of the intermolecular bonding contrast is not yet understood. Nevertheless, the images leave no doubt that STHM records a genuine surface property of the two molecular layers that we have studied in which local intermolecular bonds leave a mark. This property can be, e.g., the electron density, electric fields, or the interaction potential between the surface and the hydrogen molecule(s) in the junction that are used for STHM imaging. Once we know more about the contrast mechanism, even quantitative details of intermolecular interactions may become accessible by STHM.

Supporting Information Available: A larger section of Figure 2e. This material is available free of charge via the Internet at http://pubs.acs.org.

References

(1) Barlow, S. M.; Raval, R. *Surf. Sci. Rep.* **2003**, *50*, 201.
(2) Ueno, N.; Kera, S. *Prog. Surf. Sci.* **2008**, *83*, 490.
(3) Kraft, A.; Temirov, R.; Henze, S. K. M.; Soubatch, S.; Rohlfing, M.; Tautz, F. S. *Phys. Rev. B* **2006**, *74*, 041402.
(4) Kilian, L.; Hauschild, A.; Temirov, R.; Soubatch, S.; Schöll, A.; Bendounan, A.; Reinert, F.; Lee, T.-L.; Tautz, F. S.; Sokolowski, M.; Umbach, E. *Phys. Rev. Lett.* **2008**, *100*, 136103.
(5) Temirov, R.; Soubatch, S.; Neucheva, O.; Lassise, A. C.; Tautz, F. S. *New J. Phys.* **2008**, *10*, 053012.
(6) Weiss, C.; Wagner, C.; Kleimann, C.; Rohlfing, M.; Tautz, F. S.; Temirov, R. Accepted for publication in *Phys. Rev. Lett.* (cond-mat arXiv:1006.0835v2).
(7) Kilian, L.; Umbach, E.; Sokolowski, M. *Surf. Sci.* **2006**, *600*, 2633.
(8) Tautz, F. S. *Prog. Surf. Sci.* **2007**, *82*, 479. and references therein.
(9) Seidel, C.; Awater, C.; Liu, X. D.; Ellerbrake, R.; Fuchs, H. *Surf. Sci.* **1997**, *371*, 123. and references therein.
(10) Mura, M.; Sun, X.; Silly, F.; Jonkman, H. T.; Briggs, G. A. D.; Castell, M. R.; Kantorovich, L. N. *Phys. Rev. B* **2010**, *81*, 195412.
(11) Steiner, T. *Angew. Chem.* **2002**, *114*, 50.
(12) Kröger, J.; Jensen, H.; Berndt, R.; Rurali, R.; Lorente, N. *Chem. Phys. Lett.* **2007**, *438*, 249.
(13) Mannsfeld, S.; Toerker, M.; Schmitz-Hübsch, T.; Sellam, F.; Fritz, T.; Leo, K. *Org. Electron.* **2001**, *2*, 121.
(14) Neumann, A.; Schroeder, S. L. M.; Christmann, K. *Phys. Rev. B* **1995**, *51*, 17007.
(15) Shannon, R. D. *Acta Crystallogr., Sect. A* **1976**, *32*, 751.
(16) Bondi, A. *J. Phys. Chem.* **1964**, *68*, 441.
(17) Ogawa, T.; Kuwamoto, K.; Isoda, S.; Kobayashi, T.; Karl, N. *Acta Crystallogr., Sect. B* **1999**, *55*, 123.

JA104332T